A Wideband Series-Fed Circularly Polarized Differential Antenna by Using Crossed Open Slot-Pairs

Le-Hu Wen, Steven Gao, *Fellow, IEEE*, Qi Luo, *Senior Member, IEEE*, Qingling Yang, Wei Hu, *Member, IEEE*, Yingzeng Yin, *Member, IEEE*, Jian Wu, and Xiaofei Ren

***Abstract*—A novel method of designing a wideband series-fed circularly polarized (CP) differential antenna by using crossed open slot-pairs is presented in this paper. The near-field distributions and input impedance analyses show that the closely spaced open slot-pairs can radiate as the crossed dipoles and have stable radiating resistance with a compact radiator size. Besides, a wideband half-power phase shifter by using open slot is proposed and utilized to realize CP radiation. The proposed CP antenna is composed of a wide slot-pair and a narrow slot-pair. In the antenna design, the narrow slot-pair is not only excited as a radiator, but also elaborately loaded to provide wideband half-power output and quadrature phase excitation to the wide slot-pair. Both the proposed half-power phase shifter and CP antenna are illustrated by the corresponding equivalent circuits. Based on these analyses, the proposed antenna is designed, fabricated and measured. Compared to the simulated traditionally designed counterpart, 2.1 times wider axial ratio bandwidth is achieved for the proposed antenna. The measured overlapped bandwidth for axial ratio <3 dB and return loss >10 dB is 1.95-3.45 GHz (55.6%). Also, the antenna gain and radiation patterns are measured, which agree well with the simulated results.**

***Index Terms*—Circularly polarized antenna, differential antenna, series-fed, wideband antenna.**

I. Introduction

With the rapid development of the modern wireless communication technologies, circularly polarized (CP) antennas have been drawn increasing popularity in many applications, such as satellites, radars, and global positioning systems. Compared to the linear polarized antennas, CP antennas have the advantages of the reduced multipath effect and the flexible orientation angle between the receiving and transmitting antennas [1]. In addition to the traditional bandwidth requirements like the linearly polarized antennas, such as the impedance bandwidth, gain, beamwidth, etc., axial ratio (AR) is a unique specification for CP antennas, which usually limits the available bandwidth of the CP antennas.

To realize CP antennas, a convenient method is to generate two orthogonal degenerated radiating modes on the same radiating patch [2]-[3] with the single feed. However, it is difficult to obtain wide AR bandwidth by utilizing single feed method. To further increase the AR bandwidth of the CP antennas, two feeds [4]-[5] and four feeds [6] techniques are utilized with the help of additional wideband feed network for equal magnitude and quadrature phase excitations. Recently, by introducing quadrature coupling paths from the resonators into the radiating patch, filtering antennas with enhanced AR bandwidth are presented in [7]-[8]. However, due to the low profile configuration and high quality factor, these patch antennas usually face the problems of limited impedance and AR bandwidth, which limit the applications of these CP patch antennas.

To further improve the bandwidth of CP antennas, dipole antennas [9]-[14] are employed with a ground plane as the reflector for unidirectional radiation. In [9]-[11], by modifying the ground planes or the backed cavities, crossed dipoles are realized for wideband CP radiation. Two pairs of the off-center-fed dipoles in [12] are used to achieve broadband circular polarization. Crossed dual-dipoles [13]-[14] are presented to realize wideband CP antennas. However, most of these dipole antennas are with relatively large radiator size. In the array design, large radiator size will lead to the large element distance and strong coupling between the antenna elements. Both of these two effects are undesirable for the array design, especially for the array with the requirement of beam scanning performance [15]. Recently, with the development of the differential microwave circuit systems, differentially fed antennas become increasingly popular because they can directly match the balanced differential circuits without the need of additional baluns for signal conversion [16]. Therefore, differentially fed CP antennas [17]-[19] are developed to directly match the differential circuit systems.

In this paper, a novel method of designing a wideband series-fed CP differential antenna is presented. The antenna is composed of two crossed open slot-pairs, which can be equivalent as two crossed dipoles based on analysis of the near-field electric and magnetic field distributions. By studying the input impedance of the crossed open slot-pairs, stable radiating resistance and compact radiator size can be realized. To obtain sequential excitation with the equal magnitude and quadrature phase for CP radiation, a wideband half-power

This work was supported in part by China Research Institute of Radiowave Propagation, in part by EPSRC grants EP/N032497/1, EP/P015840/1, and EP/S005625/1, and in part by China Scholarship Council. *(Corresponding author: Le-Hu Wen.)*

L.-H. Wen, S. Gao, Q. Luo, and Q. Yang are with the School of Engineering and Digital Arts, University of Kent, Canterbury, CT2 7NT, U.K. (e-mail: lw347@kent.ac.uk)

W. Hu and Y. Yin are with the National Key Laboratory of Antennas and Microwave Technology, Xidian University, Xian, 710071, China.

J. Wu and X. Ren are with the Innovation and Research Center, China Research Institute of Radiowave Propagation, Qingdao, 266107, China.

This article has been accepted for publication in a future issue of this journal, but has not been fully edited. Content may change prior to final publication. Citation information: DOI 10.1109/TAP.2019.2951994, IEEE Transactions on Antennas and Propagation

phase shifter is realized by loading an open slot under the feed line. Based on the analyses of the crossed slot-pairs and wideband half-power shifter, the presented wideband CP antenna is developed by serially exciting the narrow open slot-pair and the wide open slot-pair. For the traditional series-fed CP antennas in [20]-[23], the impedance and AR bandwidths of these antennas are always limited by the series-fed method. Whereas in this design, the narrow open slot-pair is serially loaded not only as the radiator, but also to provide wideband equal magnitude and quadrature phase excitation for the last stage wide open slot-pair. Both the proposed wideband half-power phase shifter and the antenna are extensively analyzed and discussed based on the equivalent circuits. To verify the above design concept, the proposed antenna is fabricated and measured. The measured results of S-parameters and radiation patterns agree well with the simulated results. The overlapped bandwidth for AR<3 dB and return loss>10 dB is from 1.95 GHz to 3.45 GHz (55.6%), which is 2.1 times wider than the simulated results of the traditionally designed counterpart.

II. Design Principles

Before the design of the proposed CP antenna, two important design principles are discussed and elaborated in this section as the basis of the antenna design. The first is the crossed open slot-pairs as the main radiating structure. Then, it is followed by the half-power phase shifter as both the radiating and feeding structure.

A. Crossed Open Slot-Pairs

In this work, wideband CP radiation is realized by using two pairs of closely spaced, orthogonal arranged open slot-pairs. The radiation of the closely spaced open slot-pairs can be equivalent as the two crossed dipoles with a stable radiating resistance. Fig. 1 shows the configuration of the proposed closely spaced open slot-pairs. The radius of the circular patch is Rp. Four symmetrical slots (slot 1, slot 2, slot 3, and slot 4) are arranged closely to each other, and have the same width Ws and length Ls. Four sequential rotated lumped ports (port 1, port 2, port 3, and port 4) are used to excite the open slots with the feed position Lf0. In the figure, the slot-pair of slot 1 and slot 3 can radiate as a dipole located along the y-axis, while the slot-pair of slot 2 and slot 4 can radiate as a dipole located along the x-axis.

Fig. 2 shows the simulated near-field electric field and magnetic field distributions when the slot-pair of slot 1 and slot 3 is excited with the same current excitation magnitude and direction. As shown in Fig. 2 (a), the electric fields start from the left part of the patch and end to the right part of the patch. Symmetrical electric field distributions are observed with regard to the x-axis and y-axis in the xy plane. In Fig. 2 (b), loop-shaped magnetic field distributions are observed around the radiating patch in the xz plane. Also, symmetric magnetic field distributions are observed with regard to the x-axis and z-axis in the xz plane. Therefore, the excited slot-pair of slot 1 and slot 3 can be equivalent as a dipole placed along the y-axis, and the equivalent Dipole-y is shown in Fig. 2 (c).

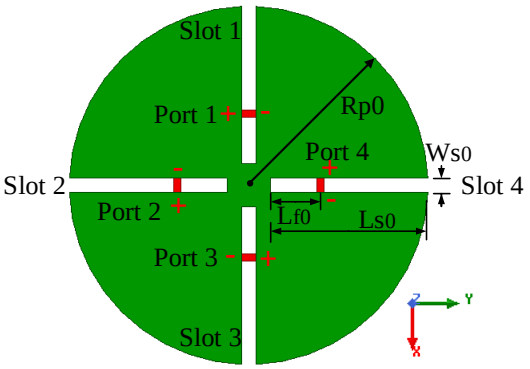

Fig. 1. Configuration of the proposed four closely spaced, orthogonal arranged crossed open slot-pairs. (Detailed parameters in the configuration: Rp0=54 mm, Ls0=24 mm, Ws0=2 mm, Lf0=6 mm.)

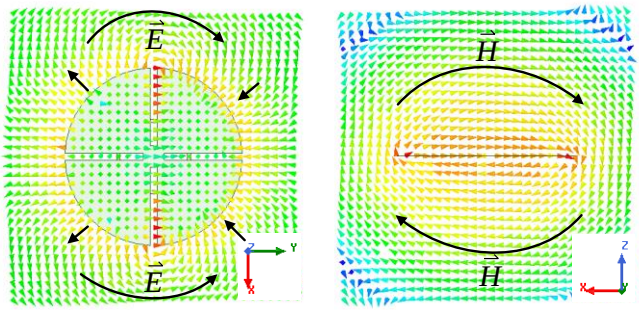

(a) (b)

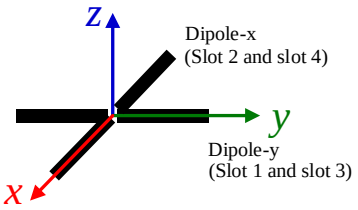

(c)

Fig. 2. Simulated near-field distribution of the antenna when the slot-pair of slot 1 and slot 3 is excited. (a) Electric field distribution. (b) Magnetic field distribution. (c) Equivalent crossed dipoles for the excited crossed slot-pairs.

Similarly, owing to the symmetry of the four open slots, same near-field distributions can be observed when the slot-pair of slot 2 and slot 4 is excited with the same excitation current magnitude and direction. The radiated electric field and magnetic field can be equivalent as the Dipole-x placed along the x-axis, which is also shown in Fig. 2 (c). When the equivalent Dipole-x and Dipole-y are excited with equal magnitude and quadrature phase signals, CP radiation will be achieved. Therefore, by exciting the crossed open slot-pairs with equal magnitude and sequential quadrature phase difference signals, ideal dipole like CP radiation patterns can be achieved.

The crossed open slot-pairs also show the stable radiating resistance and compact size when the slot width becomes wider. To facilitate the analysis of the input impedance of crossed slot-pairs for circular polarization, active S-parameters are used to evaluate the impedance characteristic of the slot-pairs, which take the consideration of the contributions of all the closely spaced open slot-pairs excited with equal magnitude and sequential quadrature phase signals. According to the definition

This article has been accepted for publication in a future issue of this journal, but has not been fully edited. Content may change prior to final publication. Citation information: DOI 10.1109/TAP.2019.2951994, IEEE Transactions on Antennas and Propagation

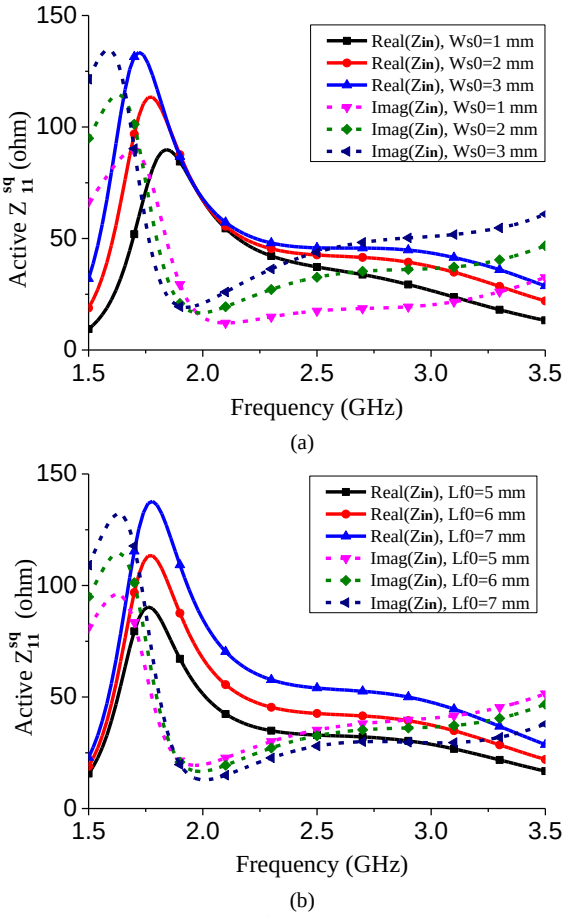

Fig. 3. Active input impedance of the crossed slot-pairs excited with equal magnitude and quadrature phase signals varies with different (a) Ws0 and (b) Lf0.

in [25], the active reflection coefficient of the N-port antenna or array can be expressed as

$$Active\ S_{11} = \sum_{i=1}^{N} \frac{a_i}{a_1} S_{1i} \tag{1}$$

where a_i is the excitation voltage of the ith driven source. Therefore, the active reflection coefficient for the sequentially excited crossed open slot-pairs in Fig. 1 can be expressed as

$$Active\ S_{11}^{sq} = S_{11} - S_{13} \tag{2}$$

and the active input impedance is

$$Active\ Z_{11}^{sq} = Z_0 \frac{1 + Active\ S_{11}^{sq}}{1 - Active\ S_{11}^{sq}} \tag{3}$$

where Z_0 is the impedance of the driven source.

Fig. 3 (a) shows the active input impedance of the slot-pairs varies with different widths of the slot. As shown in the figure, when the width of the slot Ws0 increases to 3 mm, the slop of the input resistance becomes moderate and stable to 50 ohm from 2 GHz to 3 GHz. This means that a stable radiating resistance and an effective radiation can be achieved when the width of the slot becomes wider. However, as the increase of Ws0, higher input inductance is observed. This will affect the impedance matching for the practical antenna design. Another important fact is that both the input resistance and reactance curves of the slot-pairs will shift to the lower frequency as the increase of Ws0. These two facts denote that, by increasing the width of the slots, a stable radiating resistance and a compact radiator size can be realized.

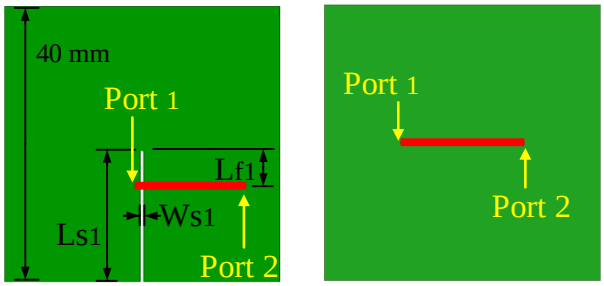

Fig. 4. (a) Configuration of the proposed half-power phase shifter. Detailed parameters: Ls1=19 mm, Ws1= 0.5 mm, Lf1= 5.9 mm. (b) The traditional microstrip phase delay line.

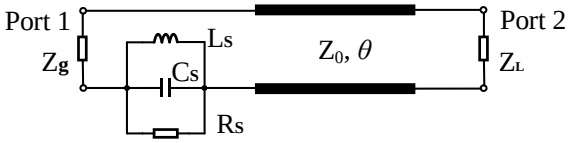

Fig. 5. Equivalent circuit of the proposed half-power phase shifter.

Fig. 3 (b) shows the input impedance of the antenna varies with different feed position Lf0. It can be seen that, as the feed position away from the center of the circular patch, the value of the input resistance increases dramatically compared to the input reactance. Therefore, by changing this parameter, the input resistance can be easily adjusted to a desired value, which can be the characteristic impedance of a coaxial cable or the other input port. In addition, both two figures in Fig. 3 (a) and Fig. 3 (b) show that the input impedance of the open slot-pairs is inductive, and the inductance increases as the frequency increases. Therefore, capacitive open-circuited stubs will be needed to compensate the inductive component of the input impedance for the practical antenna design.

B. Half-Power Phase Shifter

The open slot can be utilized to design a wideband half-power phase shifter, which is especially designed to achieve wideband half-power output and quadrature phase shift for the serially fed load. Fig. 4 (a) shows the configuration of the proposed half-power phase shifter. The commercially available Rogers 4003C substrate with the relative dielectric permittivity of 3.55 and thickness of 0.813 mm is used for the half-power phase shifter design. In the figure, a short microstrip line depicted in red colour is printed on the top layer of the substrate, and a square patch with the length of 40 mm is used as the reference ground and depicted in the green colour. A narrow slot with the width Ws1 and length Ls1 is etched on the bottom layer of the substrate. Details of other parameters are shown in the caption of Fig. 4. As a good performance comparison, a traditionally designed microstrip phase delay line without the slot loading is shown in Fig. 4 (b).

The equivalent circuit of the proposed half-power phase shifter is shown in Fig. 5. The loaded open slot can be

This article has been accepted for publication in a future issue of this journal, but has not been fully edited. Content may change prior to final publication. Citation information: DOI 10.1109/TAP.2019.2951994, IEEE Transactions on Antennas and Propagation

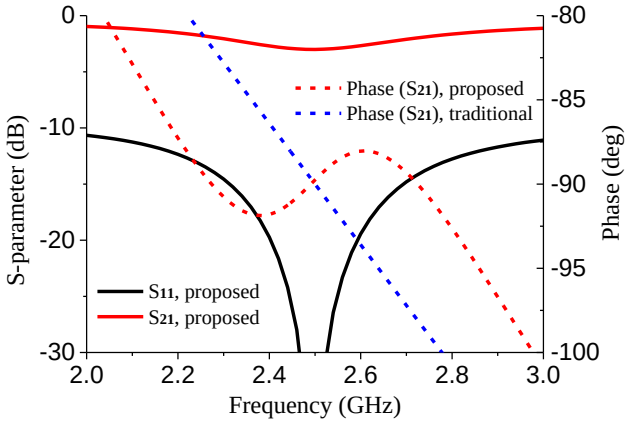

Fig. 6. Calculated frequency response of the equivalent circuit for the proposed phase shifter compared to the traditional microstrip phase delay line.

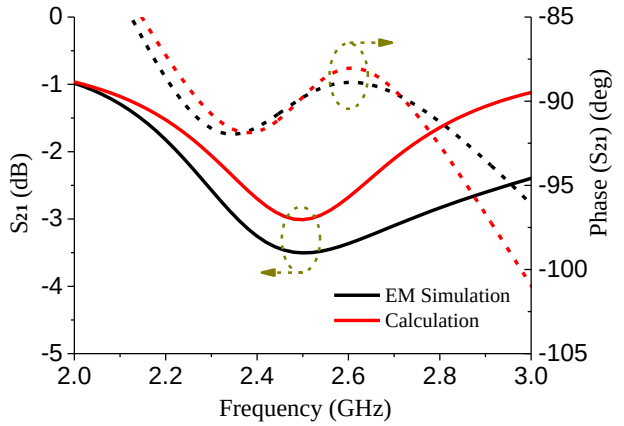

Fig. 7. EM simulated transmission magnitude and phase of the proposed half-power phase shifter compared to the calculated results.

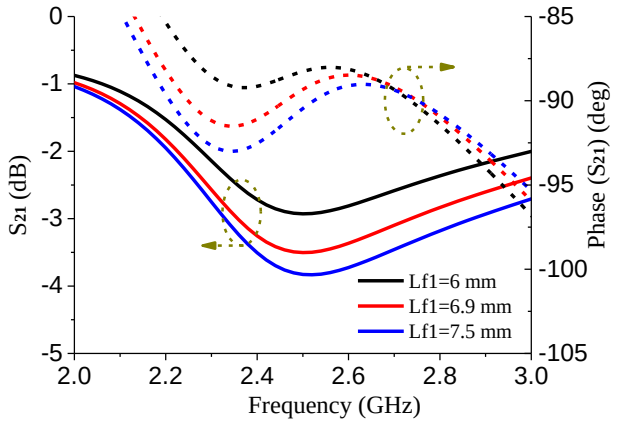

Fig. 8. Simulated transmission magnitude and phase of the proposed half-power phase shifter vary with different feed positions Lf1.

equivalent as a parallel RLC resonator with the shunt inductor L_S, capacitor C_S, and radiating resistor R_S. The resonator is serially connected to a transmission line with the characteristic impedance Z_0 and the phase θ. The impedance of generator at port 1 is Z_g, and the impedance of load at port 2 is Z_L. Based on the equivalent circuit, the ABCD matrix of this two-port network can be calculated as

$$\begin{bmatrix} A & B \\ C & D \end{bmatrix} = \begin{bmatrix} 1 & Z_S \\ 0 & 1 \end{bmatrix} \begin{bmatrix} cos\theta & jZ_0 sin\theta \\ jsin\theta/Z_0 & cos\theta \end{bmatrix} \quad (4)$$

where $Z_s = \frac{1}{\frac{1}{j\omega L_S} + j\omega C_S + \frac{1}{R_S}}$.

By converting the ABCD matrix (4) into S matrix, the reflection coefficient (S_{11}) and transmission coefficient (S_{21}) of the two-port network for the proposed half-power phase shifter with the generator impedance Z_g and load impedance Z_L can be calculated as [23]

$$S_{11} = \frac{AZ_L + B - CZ_g^* Z_L - DZ_g^*}{AZ_L + B + CZ_g Z_L + DZ_g} \quad (5)$$

$$S_{21} = \frac{2\sqrt{R_g R_L}}{AZ_L + B + CZ_g Z_L + DZ_g} \quad (6)$$

As a special case in this design, suppose that Z_L=Z_0=R_s=50 ohm, Z_L=100 ohm, the parallel RLC is resonated at 2.5 GHz, and θ equals 90º at 2.5 GHz, the frequency responses of the equivalent circuit can be then calculated by using (5)-(6). The calculated S-parameters are shown in Fig. 6. The delayed phase of the traditional microstrip line without the loading of parallel RLC is also shown in the figure for comparison.

As shown Fig. 6, a wide bandwidth of half-power output and quadrature phase is observed for the proposed phase shifter with one phase peak and one phase valley, and the bandwidth for 90±5º variance is greatly improved, which covers from 2.15 GHz to 2.86 GHz (28%). Whereas the delayed phase of the traditional microstrip line varies linearly as the frequency, and the bandwidth for 90±5º variance is very narrow, which covers only 2.36-2.64 GHz (11%). The phase bandwidth of the proposed phase shifter is 2.5 times wider than the traditional phase shifter. One should be noted is the output magnitude of this phase shifter. Half power is dissipated by the open slot, and half power is transmitted to the output port. Therefore, if another radiator is serially connected to the output port and orthogonally placed to the loaded open slot, CP radiation can be expected owing to phase and magnitude characteristics of this phase shifter.

Normally, to ensure good CP radiation, the magnitude excitations are required to be within ±0.5 dB variance, and the quadrature phase differences are required to be within ±5° variance [24]. Therefore, to achieve wider bandwidth for CP radiation, the highest insertion loss in this design can be increased to 3.5 dB, and the overlapped bandwidth for magnitude and phase will be further increased. Fig. 7 shows the EM simulated transmission magnitude and phase of the proposed half-power phase shifter. By adjusting the maximum insertion loss to 3.5 dB, the magnitude bandwidth for -3±0.5 dB is increased, as compared to the calculated result in Fig. 6. Additionally, the phase bandwidth for 90±5º is slightly increased. The overlapped simulated bandwidth for required magnitude and phase variance is 2.29-2.95 GHz (25%), which is 2.3 times wider than the traditional microstrip phase delay line.

In this work, the loaded open slot will be not only used to broaden the phase shift bandwidth, but also elaborately utilized for CP radiation. Therefore, it is important to control both the transmission coefficient and phase of the proposed half-power

This article has been accepted for publication in a future issue of this journal, but has not been fully edited. Content may change prior to final publication. Citation information: DOI 10.1109/TAP.2019.2951994, IEEE Transactions on Antennas and Propagation

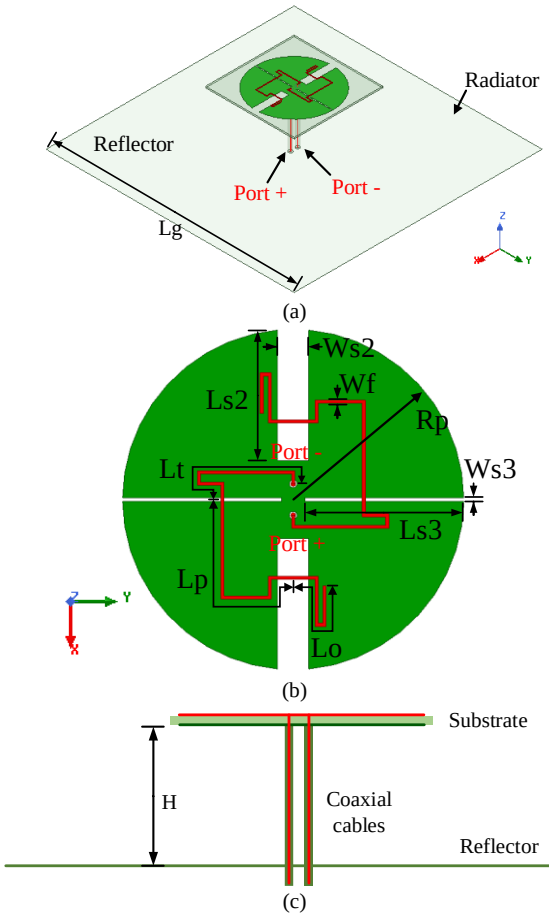

Fig. 9. Configuration of the proposed differentially fed CP antenna. (a) 3D view. (b) Detailed view of the antenna radiator. (c) Side view. (Detailed parameters of the antenna. Lg=140 mm, Ws2=4 mm, Ls2=17 mm, Ws3=0.5 mm, Ls3=20.3 mm, Rp=21.75 mm, Wf=0.4 mm, Lo=15 mm, Lp=24 mm, Lt=20 mm, H=30 mm.)

phase shifter. As shown in Fig. 8, the transmission magnitude (S_{21}) is mainly determined by the feed position Lf1. As the increase of Lf1, the transmission magnitude will be decreased. This means that more energy will be radiated by the open slot, and less energy is transmitted to output port. By changing the value of this parameter, the delayed phase is nearly unaffected. The phase bandwidth varying from -85º to -95º becomes slightly wider as Lf1 increases to 7.5 mm, but the output magnitude is decreased to -3.8 dB, which can affect the excitation magnitude of the serially fed load.

III. Antenna Design

A. Configuration

Based on the radiation and impedance characteristics of crossed slot-pairs and the proposed wideband half-power phase shifter, a wideband series-fed CP differential antenna is developed. Fig. 9 shows the detailed configuration of this antenna. In Fig. 9 (a), the antenna is composed of an antenna radiator printed on the two sides of the substrate and a planar square copper sheet as the reflector for the unidirectional radiation. Two equal length coaxial cables are used to feed the radiator and works as the differentially fed port-pair. Port+ and Port- are located at the end of the two coaxial cables to excite the antenna for CP radiation. Because of the differentially fed method, the reflection coefficient for the proposed antenna can be calculated by using the active reflection coefficient defined in (1), that is

$$S_{11}^{df} = S_{11} - S_{12} \tag{7}$$

where S_{11} and S_{12} are the single-ended S-parameters, which can be obtained from the simulated or the measured results. Then the input impedance of the differentially fed antenna is

$$Z_{11}^{df} = Z_0 \frac{1 + S_{11}^{df}}{1 - S_{11}^{df}} \tag{8}$$

where Z_0 is the impedance of the driven source.

As shown in Fig. 9 (b), two closely spaced open slot-pairs are etched on the bottom layer of the substrate and depicted in green colour. Two bent microstrip lines are rotationally printed on the top layer of the substrate and depicted in red colour. Note that the widths of crossed open slot-pairs are different, and have different functions in the antenna design. The wide slot-pair on the bottom layer with the width of Ws2 works as the main radiating structure, and is designed for the wide impedance bandwidth and compact radiator size. Whereas the narrow slot-pair with the width of Ws3 not only works as the radiating structure, but also is elaborately designed for providing the required wideband 90º phase shift to the wide slot-pair. Both of the crossed wide and narrow slot-pairs can radiate as an ideal dipole, as discussed in Section II. A. Whereas the feed lines on the top layer of the substrate, although they have the same width, they perform three totally different functions. The open-circuited stub with the length of Lo compensates the inductive component of the input impedance of the open slots for wide impedance bandwidth. The microstrip line with the length of Lp adjusts the required phase delay for circular polarization. The microstrip line with the length of Lt transforms the input impedance of the antenna into the desired characteristic impedance of the coaxial cables. Details of these working principles will be discussed in the following sections.

Fig. 9 (c) shows the side view of the antenna. A substrate of commercially available Rogers 4003C with the relative dielectric permittivity of 3.55 and the thickness of 0.813 mm is used in the antenna design. Note that the outer conductors of the cables are soldered to the bottom layer of the patch, while the inner conductors of the cables are soldered to the top layer of the bent feed lines. The distance from the substrate to the reflector is designed as 30 mm for the unidirectional CP radiation. All the simulation results in this work are obtained by using the electromagnetic simulation software ANSYS HFSS. The detailed parameters of the presented antenna are shown in the caption of Fig. 9.

B. Equivalent Circuit Analysis

To illustrate the working principle of the proposed antenna, the equivalent circuit of the proposed series-fed CP antenna is shown in Fig. 10. The wide slot and the narrow slot in the configuration of the antenna can be equivalent as the parallel RLC resonators with the radiating impedance of Z_{A1} and Z_{A2}, respectively. As shown in the figure, the input impedance Z_{in1} at the left of the narrow slot is

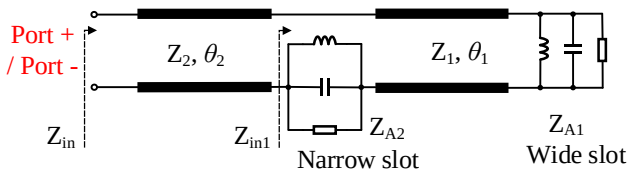

Fig. 10. Equivalent circuit of the proposed differentially fed CP antenna.

$$Z_{in1} = Z_{A2} + Z_1 \frac{Z_{A1} + jZ_1 tan\theta_1}{Z_1 + jZ_{A1} tan\theta_1} \quad (9)$$

where Z_1 and θ_1 is the characteristic impedance and electric length of microstrip line Lp. Then, the input impedance Z_{in} at the differential Port+ or Port– can be calculated as

$$Z_{in} = Z_2 \frac{Z_{in1} + jZ_2 tan\theta_2}{Z_2 + jZ_{in1} tan\theta_2} \quad (10)$$

where Z_2 and θ_2 is the characteristic impedance and electric length of microstrip line Lt.

In this design, the radiating resistor of the wide slot and narrow slot are design as 100 ohm. Therefore, the characteristic impedance of the microstrip line of Z_1 is designed also as 100 ohm, and θ_1 is required to be 90º for CP radiation. When both the wide slot and narrow slot are resonated at the same frequency, the input impedance of Z_{in1} will be 200 ohm according to (9). So an impedance inverter is needed to transform the input impedance Z_{in1} into the characteristic impedance of a coaxial cable. According to (10), a transmission line with the impedance of Z_2=100 and electric length of θ_2=90º is needed to transform the input impedance of 200 ohm into the desired 50 ohm. Although Z_1 and Z_2 are of the same values, they perform totally different functions here in the antenna design.

To further illustrate the design methods of the antenna, the evolution process of the antenna is shown in Fig. 11. Four different antennas are included in the figure. Note that all these antennas are differentially fed antennas, and have the same radiating slots at the bottom layer as the proposed antenna. In addition, same substrates and reflectors are included for these antennas in the simulation. The only differences for these antennas are the feed lines on the top layer. As shown in the figure, only wide open slot-pair is excited in Antenna 1, and two via holes are used for the direct excitation. To improve the impedance matching, open-circuited stubs are introduced in Antenna 2. Note that Antenna 1 and Antenna 2 cannot be realized for CP radiation. Therefore, to realize CP radiation, narrow open slot-pair is loaded under the top feed lines in Antenna 3, but without the impedance inverter line. The fourth antenna shown in the bottom right corner of the figure is the proposed antenna with the incorporated impedance inverter line.

Fig. 12 shows the simulated impedance characteristics of these reference antennas. In Fig. 12 (a), high inductive component is observed for the direct feed method, and the average inductance is about 100 ohm over the whole band of interest. As discussed in Section II. A, open-circuited stubs should be added to compensate the inductive component. After incorporating the open-circuited stubs into Antenna 2, the reactance of the input impedance is around 0 ohm. In addition,

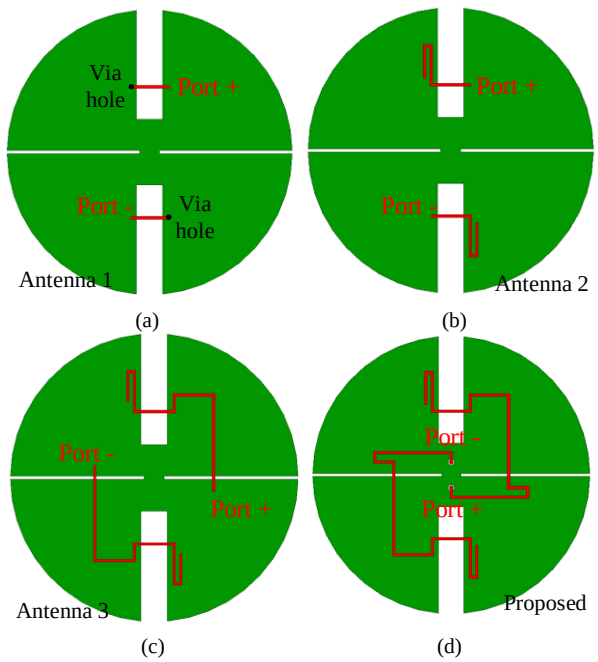

Fig. 11. Evolution of the proposed CP antenna. (a) Antenna 1 with the shorting via holes. (b) Antenna 2 with the open-circuited stubs. (c) Antenna 3 loading with the narrow slots, but without the impedance inverter line. (d) The proposed antenna.

the resistance of the input impedance is also decreased from the average value of 150 ohm to the designed average value of 100 ohm. A wide impedance bandwidth can be ensured by using the open-circuited stubs.

Fig. 12 (b) compares the simulated input impedances of Antenna 3 and the proposed antenna. As can be seen that the real part of the input impedance of Antenna 3 varies from 250 ohm to 100 ohm from 2 GHz to 3 GHz, while the imaginary part is close to zero. Therefore, an impedance inverter is needed to transform the high input resistance to the desired 50 ohm. After the impedance inverter line with the impedance of 100 ohm is incorporated into the proposed antenna, the real part of the input impedance shifts to the desired value and keeps stable around 50 ohm, while the imaginary part is still close to zero. Fig. 12 (c) shows the corresponding simulated S-parameters and ARs of the two antennas, both of the two antennas are normalized to 50 ohm. Good impedance matching can be achieved for the proposed antenna with the reflection coefficient lower than -10 dB from 1.82 GHz to 3.5 GHz. Because of the loading of the narrow open slot-pairs, both of the two antennas have almost the same wide axial ratio bandwidth, and the simulated bandwidth of the axial ratio lower than 3 dB for the proposed antenna is from 1.96 GHz to 3.41 GHz (54%).

The radiation characteristics of the evolution reference antennas are shown in Fig. 13. Fig. 13 (a) shows the simulated normalized radiation patterns of these four antennas in xz-plane at 2.5 GHz. Note that Antenna 1 and Antenna 2 are linear polarized antennas, and the only difference is that they have different feed lines. Therefore, same radiation patterns are obtained for these two antennas. In addition, it is observed that the right-hand circular polarized (RHCP) radiation pattern is same as the left-hand circular polarized (LHCP) radiation

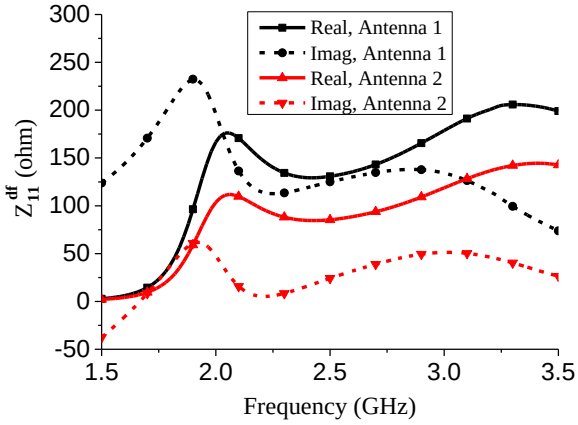

(a)

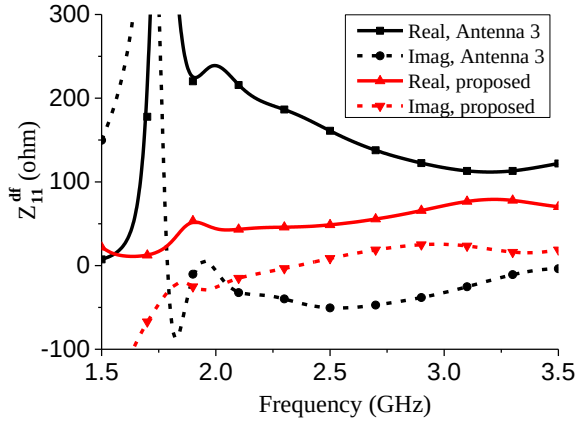

(b)

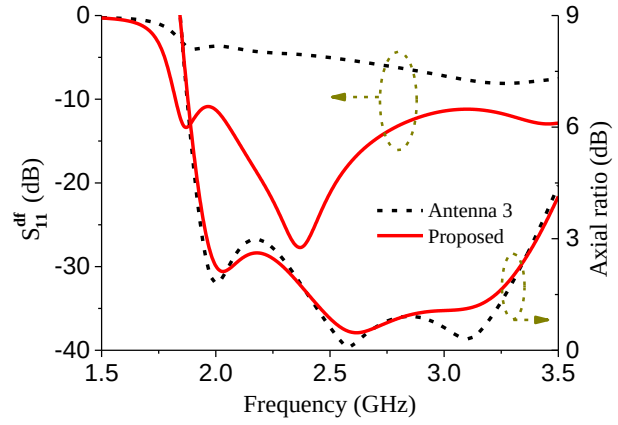

(c)

Fig. 12. (a) Input impedances of Antenna 1 and Antenna 2. (b) Input impedances of Antenna 3 and the proposed antenna. (c) S-parameters and axial ratios of Antenna 3 and the proposed antenna.

pattern for these two antennas. This is because that these two CP components are resolved from the linear polarized radiation patterns, and very high AR is obtained due to the almost same co-polarized and cross-polarized CP radiation patterns. To realize CP radiation with low AR, the narrow open slot-pair is elaborately loaded to provide equal magnitude and quadrature phase for the last stage wide open slot-pair in Antenna 3 and the proposed antenna. In addition, because the only difference between Antenna 3 and the proposed antenna is the elaborately introduced impedance inverter, the radiation patterns of them

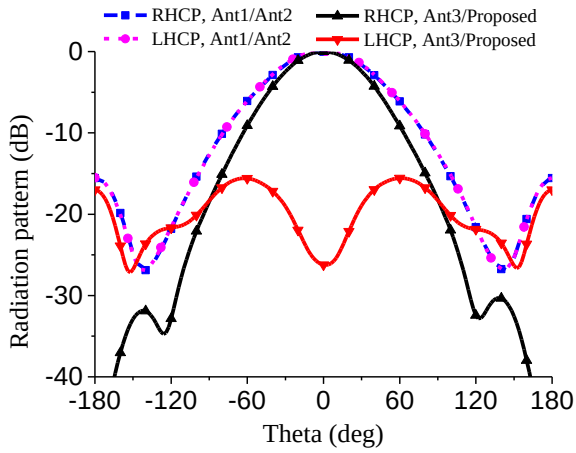

(a)

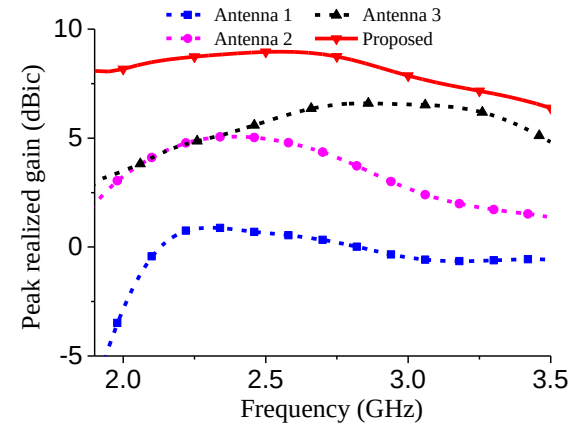

(b)

Fig. 13. Radiation characteristics of the evolution reference antennas. (a) Simulated normalized radiation patterns. (b) Peak realized gains for RHCP radiation.

are almost same. It is observed that very low cross-polarization level of -26 dB is obtained in the broadside direction at 2.5 GHz, which denotes that a very low AR is obtained at this frequency.

Fig. 13 (b) shows the simulated peak realized gains of the four antennas for RHCP radiation. All the input ports of three reference antennas are normalized to 50 ohm. Because of the high input inductance, Antenna 1 has the lowest realized RHCP gain, which is resolved from linear polarized gain. After the incorporation of the open-circuited stubs in Antenna 2, high input inductance is compensated, and the resolved realized gain for RHCP radiation is increased accordingly. However, due to same co-polarized and cross-polarized CP radiation patterns shown in Fig. 13 (a), these two antennas radiate linear polarized waves. After the loading of the narrow open slot-pair in Antenna 3, CP radiation is realized with the gain further increased at the upper band. However, due to the high input resistance at the lower band, the gain at the lower band is relatively lower. Finally, after the impedance inverter is incorporated into the proposed antenna, the input impedance is further improved and the peak realized gain at the lower band is therefore increased.

The proposed antenna has a wider axial ratio bandwidth than the traditionally designed counterpart. Fig. 14 (a) shows the configuration of traditional designed Antenna 4, which is also designed as a differentially fed antenna. Different from the

This article has been accepted for publication in a future issue of this journal, but has not been fully edited. Content may change prior to final publication. Citation information: DOI 10.1109/TAP.2019.2951994, IEEE Transactions on Antennas and Propagation

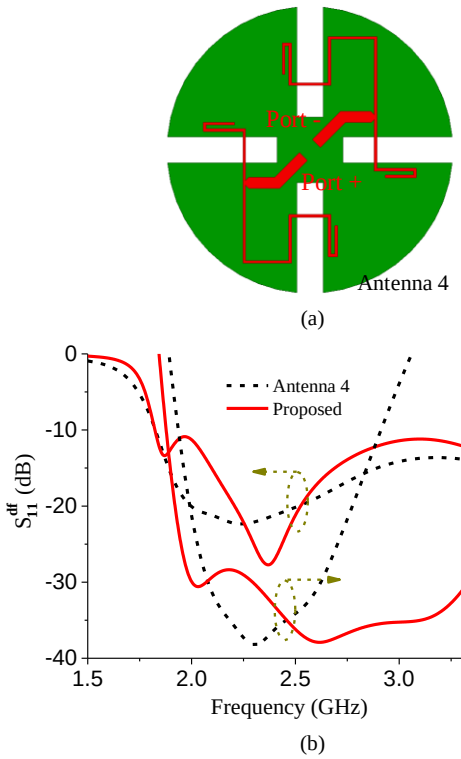

Fig. 14. Comparison to the traditionally designed CP counterpart (Antenna 4). (a) Simulation model of Antenna 4. (b) Simulated results of the two antennas.

proposed antenna, only wide slots are used in Antenna 4. A traditional T-shaped power divider and two bent microstrip lines are used for the required magnitude and phase excitations for CP radiation. Fig. 14 (b) shows the simulated S-parameters and axial ratios of these two antennas. As compared to Antenna 4, the reflection coefficient of the proposed CP antenna is slightly higher. However, it is still very good and lower than -10 dB from 1.82 GHz to 3.5 GHz. Most importantly, much wider axial ratio bandwidth is observed for the proposed antenna, which is from 1.96 GHz to 3.41 GHz (54%) for AR<3 dB. Whereas the AR bandwidth for Antenna 4 is quite narrow, which is only from 2.05 GHz to 2.67 GHz (26%). The overlapped bandwidth of impedance and AR limits the application of Antenna 4 for CP radiation. Compared to Antenna 4, 2.1 times wider relative AR bandwidth is achieved for the proposed antenna by using the proposed design method. The simulated AR bandwidth enhancement also agrees well with the simulated magnitude and phase bandwidth enhancement of the proposed half-power phased shifter, as compared to the traditional microstrip phase shift line shown in Fig. 4.

IV. Results and Discussion

A. Antenna Verification

To validate the antenna design concept, the proposed differentially fed CP antenna was designed, fabricated, and measured. Fig. 15 shows the photographs of the fabricated prototype and the prototype under test. The antenna was measured by the Anritsu 37397C vector network analyzer and ASYSOL far field antenna measurement system at University of Kent. Fig. 16 shows the simulated and measured

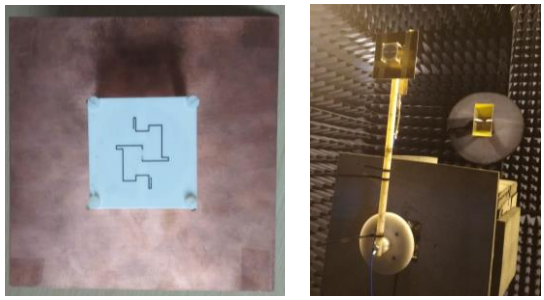

Fig. 15. Photographs of (a) the fabricated prototype of the proposed differentially fed CP antenna and (b) the prototype under radiation pattern test.

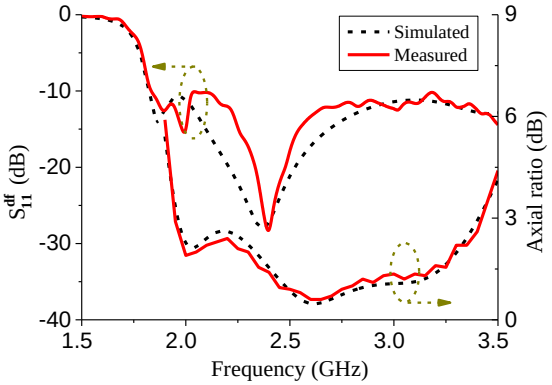

Fig. 16. Measured and simulated S-parameters and axial ratios of the proposed differentially fed CP antenna.

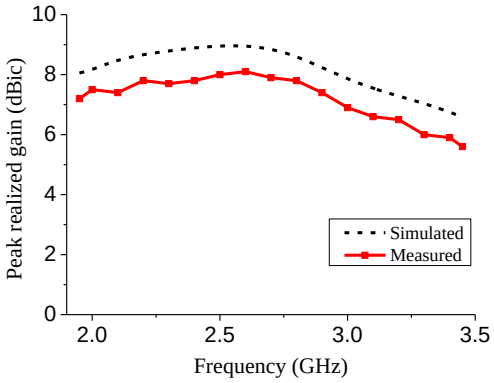

Fig. 17. Measured and simulated peak realized gain of the proposed differentially fed CP antenna.

S-parameters and axial ratios of the proposed differentially fed CP antenna. The measured reflection coefficient from 1.84 GHz to 3.5 GHz is below -10 dB, and the measured AR below 3 dB is from 1.95 GHz to 3.45 GHz. The overlapped relative bandwidth for the reflection coefficient and AR is 55.6%. Both the measured S-parameters and AR agree well with the simulated results. The slight discrepancies between the simulated and measured results are possibly due to the fabrication and solder errors between the radiator and the coaxial cables.

The measured peak realized CP radiation gain of the antenna from 1.95 GHz to 3.45 GHz is shown in Fig. 17, which is compared with the simulated result. Owing to the reflection of the reflector, high antenna gain is achieved. The measured antenna gain is about 0.9 dB lower than the simulated gain, which is probably caused by the simulation and measurement

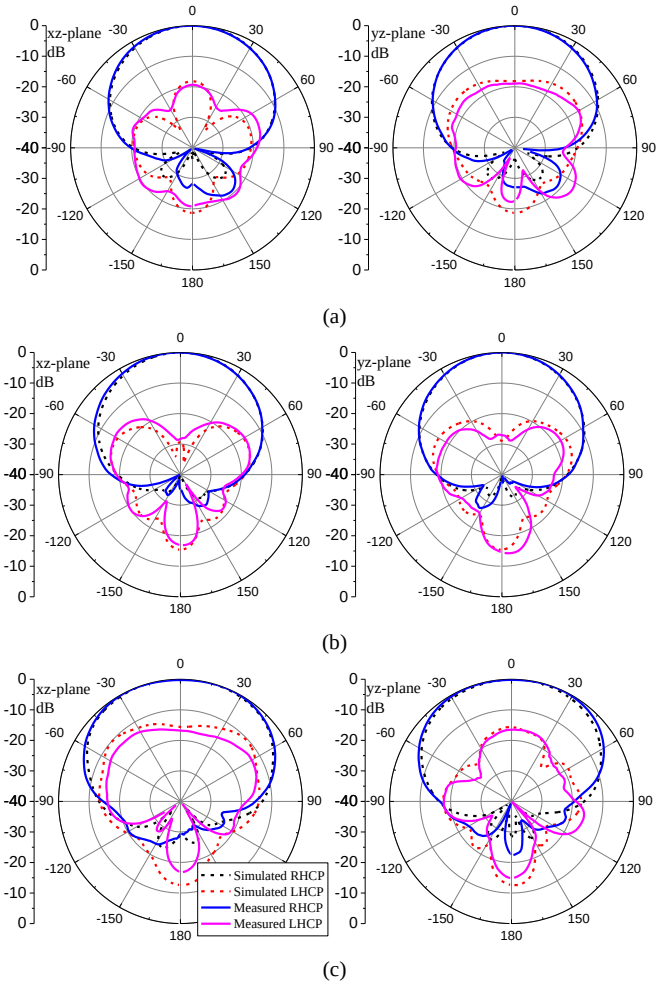

Fig. 18. Measured and simulated normalized radiation patterns of the proposed CP antenna in xz-plane and yz-plane at (a) 2 GHz, (b) 2.7 GHz, and (c) 3.4 GHz.

errors. The measured peak realized gain varies from 5.6 dBic to 8.1 dBic within the bandwidth. Fig. 18 shows the measured and simulated normalized radiation patterns of the proposed CP antenna in xz-plane and yz-plane at 2 GHz, 2.7 GHz, and 3.4 GHz. As shown in the figure, RHCP radiation is achieved in the broadside direction of the antenna, and the LHCP radiation is the cross-polarization for the antenna. Good accordance is observed between the measured and simulated radiation patterns. The measured half-power beamwidth increases from 70° to 110° in xz-plane, and increases from 68° to 112° in yz-plane. Because of the increase of the beamwidth of the radiation patterns, lower antenna gain is achieved at the upper band, as compared to the antenna gain at the lower band. Because of the reflection of the reflector, low back-lobe level is achieved, and the measured front-to-back ratio is higher than 14.5 dB with unidirectional radiation patterns. The slight discrepancies between the measured and simulated radiation patterns may be caused by the position errors of the antenna and the blockage of the feeding cables.

B. Comparison

Table I compares the presented CP antenna with the recently published CP antennas. In the table, λ_0 is the free space wavelength at the center operation frequency. As can be seen,

TABLE I
COMPARISON OF THE RECENTLY PUBLISHED CP ANTENNAS

Ref.	Overlapped BW (GHz)	f_0 (GHz)	RBW	Radiator Size	Height	Reflector Size	Gain (dBic)
[9]	2.0-4.0	3.0	66.7%	$0.86\times0.86\lambda_0^2$	$0.36\lambda_0$	$0.86\times0.86\lambda_0^2$	7.1-9.7
[10]	1-2.87	1.93	96.6%	$0.7\times0.7\lambda_0^2$	$0.35\lambda_0$	$1.5\times1.5\lambda_0^2$	~6
[11]	0.92-3.0	1.96	106%	$0.6\times0.6\lambda_0^2$	$0.24\lambda_0$	$0.6\times0.6\lambda_0^2$	~5
[12]	1.69-3.0	2.35	55%	$0.67\times0.67\lambda_0^2$	$0.32\lambda_0$	$1.59\times1.59\lambda_0^2$	6-9
[14]	1.2-1.97	1.59	47.8%	$0.61\times0.61\lambda_0^2$	$0.26\lambda_0$	$0.74\times0.74\lambda_0^2$	~6
[19]	1.7-2.38	2.06	31.1%	$0.38\times0.38\lambda_0^2$	$0.25\lambda_0$	$0.95\times0.95\lambda_0^2$	~6.5
This work	1.95-3.45	2.69	55.6%	$0.38\times0.38\lambda_0^2$	$0.27\lambda_0$	$1.26\times1.26\lambda_0^2$	5.6-8.1

the height of the proposed antenna is $0.27\lambda_0$, which is a medium height as compared to other reference antennas. A planar square ground plane with a moderate size of $1.26\times1.26\lambda_0^2$ is designed for unidirectional CP radiation. Antennas in [9]-[11] have much wider overlapped AR and impedance bandwidth than the other antennas. However, all of these antennas have modified ground structures, such as the stair-shaped cavity [9], the crossed fin-shaped cavity [10], and the rotated shorted metal plates [11], which are bulky and difficult to be extended into the antenna array designs. The antenna reported in [12] have the similar relative bandwidth compared to the presented antenna, but the electric size of the radiator is much larger. The antenna designed in [19] has the same electric size of the radiator as compared to the presented antenna, but its relative bandwidth is much narrower. By using crossed open slot-pairs for CP radiation, a compact radiator size of $0.38\lambda_0\times0.38\lambda_0$ is realized. Owing to the simple and planar reflector, the antenna can be easily extended to large array design. Furthermore, the elaborately introduced narrow slot-pair is not only excited as a radiator, but also elaborately loaded as a wideband half-power phase shifter to provide wideband magnitude and phase excitation to the wide slot-pair. Therefore, wide overlapped bandwidth (55.6%) and compact radiator size is achieved for the presented antenna.

V. CONCLUSION

This paper presents a novel method of designing a wideband series-fed differential CP antenna by using crossed slot-pairs. The radiation of the slot-pairs can be equivalent as the crossed dipoles, and have stable radiating resistance with a compact radiator size. In addition, by loading an open slot, a wideband half-power phase shifter is proposed and utilized to design the CP antenna. The presented antenna is composed of a wide slot-pair and a narrow slot-pair. By serially exciting the crossed slot-pairs, CP radiation is realized. In the antenna design, the narrow slot-pair not only works as a radiator, but also is elaborately loaded as a wideband half-power shifter to provide quadrature phase shift and equal magnitude for the last stage wide slot-pair. The working principles of the wideband half-power phase shifter and the proposed antenna are illustrated by their equivalent circuits. Based on these analyses, the proposed CP antenna was fabricated and measured. Compared to the simulated traditionally designed counterpart, 2.1 times wider overlapped bandwidth for impedance and AR is measured, which is from 1.95 GHz to 3.45 GHz (55.6%). The

presented wideband CP antenna can be a good candidate for wireless communications.

REFERENCES

[1] K. L. Lau and K. M. Luk, "A novel wide-band circularly polarized patch antenna based on L-probe and aperture-coupling techniques," *IEEE Trans. Antennas Propag.*, vol. 53, no. 1, pp. 577-582, Jan. 2005.

[2] Y. Shi and J. Liu, "A circularly polarized octagon-star-shaped microstrip patch antenna with conical radiation pattern," *IEEE Trans. Antennas Propag.*, vol. 66, no. 4, pp. 2073-2078, April 2018.

[3] Nasimuddin, Z. N. Chen and X. Qing, "A compact circularly polarized cross-shaped slotted microstrip antenna," *IEEE Trans. Antennas Propag.*, vol. 60, no. 3, pp. 1584-1588, March 2012.

[4] A. Narbudowicz, X. Bao and M. J. Ammann, "Dual circularly-polarized patch antenna using even and odd feed-line modes," *IEEE Trans. Antennas Propag.*, vol. 61, no. 9, pp. 4828-4831, Sept. 2013.

[5] Q. Liu, J. Shen, H. Liu and Y. Liu, "Dual-band circularly-polarized unidirectional patch antenna for RFID reader applications," *IEEE Trans. Antennas Propag.*, vol. 62, no. 12, pp. 6428-6434, Dec. 2014.

[6] L. Bian, Y. X. Guo, L. C. Ong and X. Q. Shi, "Wideband circularly-polarized patch antenna," *IEEE Trans. Antennas Propag.*, vol. 54, no. 9, pp. 2682-2686, Sept. 2006.

[7] C. Mao, S. S. Gao, Y. Wang and J. T. Sri Sumantyo, "Compact broadband dual-sense circularly polarized microstrip antenna/array with enhanced isolation," *IEEE Trans. Antennas Propag.*, vol. 65, no. 12, pp. 7073-7082, Dec. 2017.

[8] Q. Wu, X. Zhang and L. Zhu, "A wideband circularly polarized patch antenna with enhanced axial ratio bandwidth via co-design of feeding network," *IEEE Trans. Antennas Propag.*, vol. 66, no. 10, pp. 4996-5003, Oct. 2018.

[9] T. K. Nguyen, H. H. Tran and N. Nguyen-Trong, "A wideband dual-cavity-backed circularly polarized crossed dipole antenna," *IEEE Antennas Wireless Propag. Lett.*, vol. 16, pp. 3135-3138, 2017.

[10] L. Zhang *et al*., "Single-feed ultra-wideband circularly polarized antenna with enhanced front-to-back ratio," *IEEE Trans. Antennas Propag.*, vol. 64, no. 1, pp. 355-360, Jan. 2016.

[11] Y. M. Pan, W. J. Yang, S. Y. Zheng and P. F. Hu, "Design of wideband circularly polarized antenna using coupled rotated vertical metallic plates," *IEEE Trans. Antennas Propag.*, vol. 66, no. 1, pp. 42-49, Jan. 2018.

[12] R. Li, L. Pan and Y. Cui, "A novel broadband circularly polarized antenna based on off-center-fed dipoles," *IEEE Trans. Antennas Propag.*, vol. 63, no. 12, pp. 5296-5304, Dec. 2015.

[13] Y. Luo, Q. Chu and L. Zhu, "A low-profile wide-beamwidth circularly-polarized antenna via two pairs of parallel dipoles in a square contour," *IEEE Trans. Antennas Propag.*, vol. 63, no. 3, pp. 931-936, March 2015.

[14] R. Xu, J. Li and W. Kun, "A broadband circularly polarized crossed-dipole antenna," *IEEE Trans. Antennas Propag.*, vol. 64, no. 10, pp. 4509-4513, Oct. 2016.

[15] C.A. Balanis, *Antenna Theory: Analysis and Design*, John Wiley, 3rd edition, 2005.

[16] Z. Tang, J. Liu, Y. Cai, J. Wang and Y. Yin, "A wideband differentially fed dual-polarized stacked patch antenna with tuned slot excitations," *IEEE Trans. Antennas Propag.*, vol. 66, no. 4, pp. 2055-2060, April 2018.

[17] W. Chen, H. Chen, C. Lee and C. G. Hsu, "Differentially fed wideband circularly polarized slot antenna," *IEEE Trans. Antennas Propag.*, vol. 67, no. 3, pp. 1941-1945, March 2019.

[18] X. Ruan and C. H. Chan, "A circularly polarized differentially fed transmission-line-excited magnetoelectric dipole antenna array for 5G applications," *IEEE Trans. Antennas Propag.*, vol. 67, no. 3, pp. 2002-2007, March 2019.

[19] Z. Tu, K. Jia and Y. Liu, "A differentially fed wideband circularly polarized antenna," *IEEE Antennas Wireless Propag. Lett.*, vol. 17, no. 5, pp. 861-864, May 2018.

[20] A. T. Castro and S. K. Sharma, "Inkjet-printed wideband circularly polarized microstrip patch array antenna on a pet film flexible substrate material," *IEEE Antennas Wireless Propag. Lett.*, vol. 17, no. 1, pp. 176-179, Jan. 2018.

[21] Y. Yang, J. Guo, B. Sun, Y. Cai and G. Zhou, "The design of dual circularly polarized series-fed arrays," *IEEE Trans. Antennas Propag.*, vol. 67, no. 1, pp. 574-579, Jan. 2019.

[22] Y. Yang, B. Sun and J. Guo, "A low-cost, single-layer, dual circularly polarized antenna for millimeter-wave applications," *IEEE Antennas Wireless Propag. Lett.*, vol. 18, no. 4, pp. 651-655, April 2019.

[23] D. A. Frickey, "Conversions between S, Z, Y, H, ABCD, and T parameters which are valid for complex source and load impedances," *IEEE Trans. Microw. Theory Techn.*, vol. 42, no. 2, pp. 205-211, Feb. 1994.

[24] Y. Guo, K. Khoo and L. C. Ong, "Wideband circularly polarized patch antenna using broadband baluns," *IEEE Trans. Antennas Propag.*, vol. 56, no. 2, pp. 319-326, Feb. 2008.

[25] D. M. Pozar, "The active element pattern," *IEEE Trans. Antennas Propag.*, vol. 42, no. 8, pp. 1176-1178, Aug. 1994.

Le-Hu Wen received the M.S. degree in Xidian University, Xi'an, China, in 2011. He is currently working toward the Ph.D. degree with the University of Kent, Canterbury, U.K. His current research interests include multi-band base station antenna, mobile terminal antenna, and tightly coupled array.

Steven Gao (M'01–SM'16-F'19) received the Ph.D. degree in microwave engineering from Shanghai University, Shanghai, China, in 1999.

He is currently a Full Professor and Chair in RF and Microwave Engineering, and the Director of Graduate Studies at the School of Engineering and Digital Arts, University of Kent, UK. His current research interests include smart antennas, phased arrays, MIMO, satellite antennas, satellite communications, UWB radars, synthetic aperture radars, and mobile communications. He is currently an Associate Editor of the IEEE TRANSACTIONS ON ANTENNAS AND PROPAGATION.

Qi Luo (S'08–M'12-SM'19) is currently a Research Fellow with the School of Engineering and Digital Arts, University of Kent, Canterbury, U.K.

Qingling Yang is currently working toward the Ph.D. degree with the School of Engineering and Digital Arts, University of Kent, Canterbury, U.K.

Wei Hu (S'09–M'14) is currently an Associate Professor with the National Key Laboratory of Antennas and Microwave Technology, Xidian University, Xi'an, China.

Yingzeng Yin (M'16) is currently a Professor with the National Key Laboratory of Antennas and Microwave Technology, Xidian University, Xi'an, China.

Xiaofei Ren is currently a Senior Engineer with the the Innovation and Research Center, China Research Institute of Radiowave Propagation, Qingdao, China.

Jian Wu is currently the Director of the China Research Institute of Radiowave Propagation with the the Innovation and Research Center, China Research Institute of Radiowave Propagation, Qingdao, China.